

YALE PEABODY MUSEUM

P.O. BOX 208118 | NEW HAVEN CT 06520-8118 USA | PEABODY.YALE. EDU

JOURNAL OF MARINE RESEARCH

The *Journal of Marine Research*, one of the oldest journals in American marine science, published important peer-reviewed original research on a broad array of topics in physical, biological, and chemical oceanography vital to the academic oceanographic community in the long and rich tradition of the Sears Foundation for Marine Research at Yale University.

An archive of all issues from 1937 to 2021 (Volume 1–79) are available through EliScholar, a digital platform for scholarly publishing provided by Yale University Library at <https://elischolar.library.yale.edu/>.

Requests for permission to clear rights for use of this content should be directed to the authors, their estates, or other representatives. The *Journal of Marine Research* has no contact information beyond the affiliations listed in the published articles. We ask that you provide attribution to the *Journal of Marine Research*.

Yale University provides access to these materials for educational and research purposes only. Copyright or other proprietary rights to content contained in this document may be held by individuals or entities other than, or in addition to, Yale University. You are solely responsible for determining the ownership of the copyright, and for obtaining permission for your intended use. Yale University makes no warranty that your distribution, reproduction, or other use of these materials will not infringe the rights of third parties.



This work is licensed under a Creative Commons Attribution-NonCommercial-ShareAlike 4.0 International License.
<https://creativecommons.org/licenses/by-nc-sa/4.0/>



Gulf of Maine Intermediate Water

by T. S. Hopkins¹ and N. Garfield III²

ABSTRACT

The thermohaline dynamics of the Gulf of Maine are analyzed from the two year, eight cruise, data set of Colton, Marak, Nickerson, and Stoddard (1968). Six water masses are described: the Maine Surface Water, Maine Intermediate Water, and the Maine Bottom Water as interior water masses; and the Scotian Shelf Water, the Slope Water, and the Georges Bank Water as exterior water masses. Particular attention is given to the formation and disposition of the Maine Intermediate Water. Salt balance, *T-S* volume, and *T-S* drift analyses are used to provide transport and mixing estimates for the year 1966. The Slope Water entered at depth through the Northeast Channel at a rate of 2600 km³/yr; while the Scotian Shelf Water entered the surface and intermediate layers, mostly during winter intrusions, at a rate of 5200 km³/yr. The surface and intermediate layers exported a total of 7900 km³/yr in a 3:5 ratio, respectively. The Maine Intermediate Water tends to collect over the Wilkinson Basin during the stratified season, to exit via the Great South Channel during early spring, and to exit via the Northeast Channel during spring and summer. Comparisons are made between the estimated winter heat loss of 280 Ly/d and the observed heat losses of 230 Ly/d (surface layer) and 360 Ly/d (surface and intermediate layers). A limit for the Scotian Shelf Water contribution is about -70 Ly/d. It is concluded that the Maine Intermediate Water is produced locally and that it is exported in significant quantities.

1. Introduction

a. Features. The bathymetry and the geographic location of the Gulf of Maine are vital factors in its thermohaline dynamics. The Gulf of Maine is much more an enclosed basin than its sea level contour indicates (Fig. 1). Its surface opening to the North Atlantic is about 30% of its smoothed perimeter; at 45 m this reduces to 15%, and at 180 m to less than 2%. Georges Bank is the major bathymetric feature blocking the opening. Browns Bank on the Scotian Shelf and Nantucket Shoals also contribute to the restriction. The Northeast Channel is the only deep access with a sill depth of 230 m and a cross sectional area of about 7.5 km². The Great South Channel (70 m sill) and the shelf depression north of Browns Bank (130 m sill) are the only other accesses deeper than 50 m. Inside the Gulf, the bottom

1. Oceanographic Sciences Division, Brookhaven National Laboratory, Upton, New York, 11973, U.S.A.

2. Bigelow Laboratory for Ocean Sciences, West Boothbay Harbor, Maine, 04575, U.S.A.

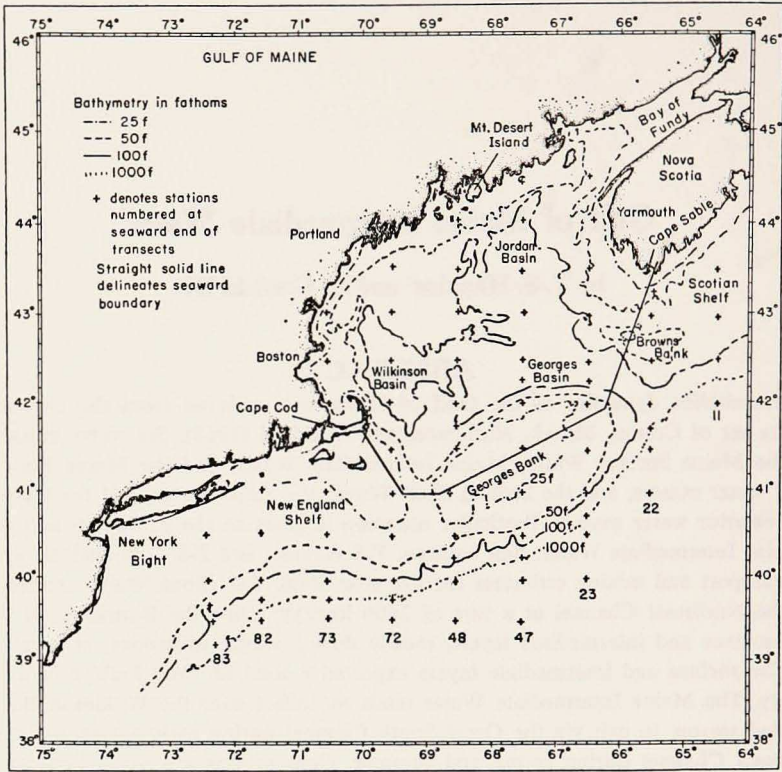


Figure 1. Bathymetry and geographic locations for Gulf of Maine. Station locations correspond to those of Colton *et al.* (1968) during the data year 1966.

topography is very uneven, but the distributions with depth of bottom area and volume are relatively constant (Fig. 2). The volume of the Gulf of Maine (14,100 km³) is about twice that of the mid-Atlantic Bight. The river discharge into the Gulf of Maine is about half the river discharge into the Middle Atlantic Bight. Meade (1971) estimated the mean discharge into the former to be 95 km³/yr while Bue (1970) computed a mean annual discharge of 157 km³ into the latter. In a geographic sense, the Gulf of Maine lies on the eastern side of the North American

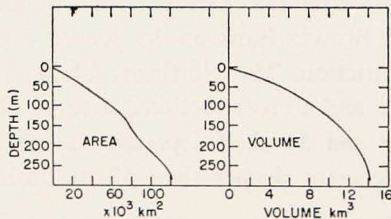


Figure 2. The area and volume of the Gulf of Maine computed using the seaward boundary of Figure 1. The area represents the horizontal projection between depth contours.

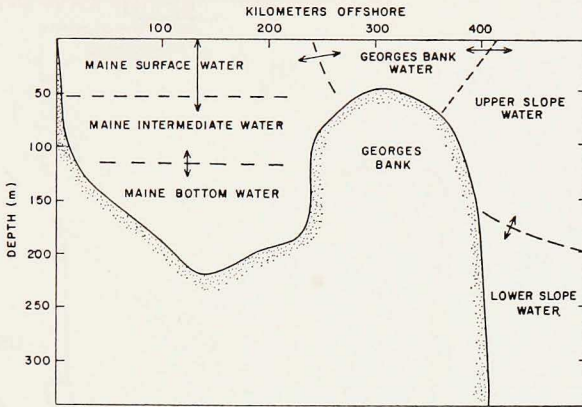


Figure 3. Cross-sectional schematic of Gulf of Maine water masses. The arrows represent variations of the water mass boundaries.

continent between the latitude band of 40 to 45N such that it experiences a high incidence of westerly continental air flow. These are some of the main physiographic features that are causal to the thermohaline response of the Gulf of Maine.

b. Background. The major observational efforts in the Gulf of Maine have occurred on several occasions: during the periods of 1912-1925, 1964-1966, 1969-1970 and 1975-present. The earliest data set has been reported by Bigelow (1927) and still remains as the most comprehensive work. Other interpretations since Bigelow have focused on such aspects as Colton's (1968) analysis of temperature trends, Bumpus and Lauzier's (1965) report on drift bottle and sea bed drifters, or Brown and Beardsley's (1978) analysis of hydrographic observations in the western Gulf of Maine. The reader is referred to Colton (1964), Bumpus (1973 and 1976), and to Hopkins and Garfield (1978) for more detailed reviews. This work is an analysis of the 1964-1966 data set as compiled by Colton *et al.* (1968); and it concentrates on the intermediate water mass.

c. Significance. The Gulf of Maine Intermediate Water (MIW) is a seasonally variable water mass produced during winter. It is replenished each winter by atmospheric buoyancy extraction processes; and during the remainder of the year, it is altered by mixing and is diminished by export. The winter cold water production normally is not sufficient to fill the entire Gulf of Maine basin. The water mass below the MIW is warmer and saltier, the Maine Bottom Water (MBW). During the stratified seasons, the MIW is overlain by the Maine Surface Water (MSW) which is produced as a consequence of net buoyancy addition to the surface. The MIW shows up as a temperature minimum in the water column. The minimum temperature is bounded by the temperatures reached during its production. Figures 3 and 4 make these points more clear. The MIW is found in the 50-120 m depth range

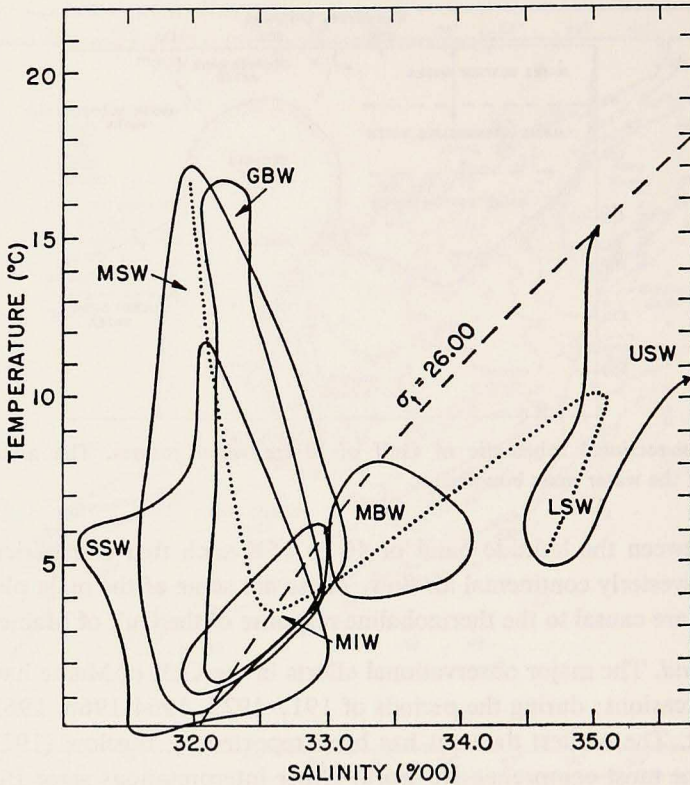


Figure 4. T - S envelopes from a composite of the Colton *et al.* (1968) data from December 1965 to September 1966. The water mass abbreviations are MSW, Maine Surface Water; MIW, Maine Intermediate Water; MBW, Maine Bottom Water; SSW, Scotian Shelf Water; GBW, Georges Bank Water; USW, Upper Slope Water; and LSW, Lower Slope Water.

(Fig. 3) and is enclosed by the water type envelope of 1-6° and 32-33‰ (Fig. 4). These ranges are schematic; they will vary depending on the season, the year, and location.

The need to focus attention on the MIW stems from two recently emerging realizations. The first of these is that the band of cooler water, constituted by the MIW, covers a large portion of the benthic regime. The exposure is roughly proportional (Fig. 2) to the vertical thickness of the MIW, which may vary from zero to more than 50% of any cross section. The geographic distribution of certain demersal fish stocks are influenced by annual trends in temperature. Colton (1972) has given evidence that detectable southward shifts occurred for the distribution of American plaice and butterfish associated with the cooling trend between 1952-1967. The 3-7°C thermal band of the MIW coincides with the optimal spawning temperatures for stocks such as plaice and haddock; and since this range differs by several degrees from that of the MSW, or even MBW, local variations in the MIW availability

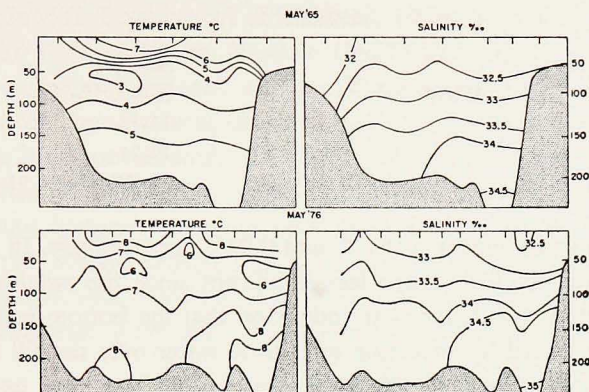


Figure 5. Gulf of Maine temperature and salinity profiles for a transect from Mt. Desert Island to Georges Bank. The 1976 data is from NMFS, 1976.

could represent significant differences in thermal regulation of the duration of spawning populations.

Bigelow (1933) labeled a cool, low-saline water mass found in the lower layer at the shelf edge of the Mid-Atlantic Bight as the "cold pool." He identified it as remnant winter water. More recent observations (e.g. Beardsley, Boicourt, and Hansen, 1976) have shown the cold pool to be moving to the southwest along the bathymetric contours. Such a movement implies an upstream source. Various possibilities have been suggested, among them the Gulf of Maine. Thus, the second realization involves the potential of the MIW as being a source for the sub-thermocline waters of the Mid-Atlantic Bight.

2. Water mass description

The existence of long term trends in water type makes difficult the statistical definition of water masses from historical data. The interior water temperatures in the Gulf of Maine, reported by Bigelow (1927), are $\sim 4^{\circ}\text{C}$ cooler than those found in recent years (NMFS, 1976). Colton (1968) identified temperature trends between the years 1940 and 1967, such that a temperature minimum existed in the early 1940's and a maximum during 1952-53. Recent data show a maximum in 1975-76. Colton's analysis showed that the subsurface trends followed those of the surface water (Boothbay Harbor), and that the deviation from the long term annual mean inside the Gulf of Maine (Wilkinson Basin) was less than for those of areas outside.

In the Gulf of Maine basin, salinity trends are associated with these temperature trends, that is, warming trends coincide with salting trends and vice versa. Comparable cross sections through the Gulf of Maine are shown for the years 1966 and 1976 in Figure 5. Over this time period the annual change in temperature and salt

Table 1

Water Mass	Stations
MSW, MIW, MBW	29-40, 55-66
SSW	13-18
SW	19-21
GBW	27, 28, 41-43, 51-54

is nearly uniform (with depth) at 0.4°C and 0.04‰ , respectively. In terms of potential energy, the variability is much less significant since the resulting T - S changes are nearly isopycnal. The latter is an indication that the bottom water densities are more directly controlled by advection of outside water over the sill than by surface production of dense water. The effects of atmospheric buoyancy extraction are not such as to cause isopycnal changes in water type. In fact, the resulting T - S drift occurring during severe cooling events is more nearly parallel to the gradient of density (e.g. Swallow and Caston, 1973, and Hopkins, 1978). External control of bottom water density classifies the Gulf of Maine as a positive basin, as suggested by Hopkins (1978). During cold years, the surface water types labelled with lower salinities have a greater opportunity for survival in the basin than do the more saline water types, which after cooling are more dense and preferentially exported from the basin.

A definition of the MIW cannot be tied to absolute temperature and salinity ranges, for reason of its relative variability. The minimum temperature water type is more easily specified than the maximum. For a given year the minimum water type falls out from T - S scatter diagrams of data from late winter and early spring. The upper bounds cannot be easily found unarbitrarily. For quantitative estimates of MIW production, this creates a problem.

The Gulf of Maine system has associated with it six water masses. These are presented in Figures 3 and 4, and are described briefly below. Three of these are interior to the Gulf: the MSW, MIW, and MBW; and three are boundary water masses: the Scotian Shelf Water (SSW), and Slope Water (SW, upper and lower), and the Georges Bank Water (GBW). For reference to the Colton *et al.* (1968) data, Table 1 gives the stations used to define the various water masses.

a. Scotian Shelf Water. For the purposes of this work the SSW is restricted to include the T - S envelope of water found on the shelf east of the transect running south from Cape Sable to the Northeast Channel. It will be noted from Figure 4 that the SSW shares a large T - S overlap with the MIW, MSW, and GBW. This is assumed to be due to similar circumstances of production. However, the SSW is distinguished by a narrower temperature range (0 - 12°C) than the MSW; and the median salinity is slightly fresher (31.8‰) than that of the MSW.

The SSW is a boundary water mass for the Gulf of Maine, and in the event of westward transport on the Scotian Shelf, a source water. Various authors (e.g.

Bigelow, 1927; Sutcliff, Loucks and Drinkwater, 1976) have suggested a transport westward into the Gulf of Maine. Bigelow (1927) suggested that SSW flows into the Gulf during spring and summer; whereas Bumpus and Lauzier (1965) described a westward flow off Cape Sable as characteristic of the winter season. Comprehensive data on the transport through the Cape Sable cross-section do not yet exist. Using data reported by Drinkwater and Sutcliff (1977), Brown and Beardsley (1978) estimated a volume transport range of $(200-300) \times 10^8 \text{m}^3 \text{sec}^{-1}$. Trites and Banks (1958) showed that surface drifters tend to recirculate on the Scotian Shelf at Cape Sable; that is, to flow west nearshore and return to the south and east off the Cape in a cyclonic, shelf-wide gyre and not necessarily to feed into the eastern Gulf of Maine.

Surface contour maps of temperature and salinity (e.g. Colton *et al.*, 1968, and Hayes, 1975) often show strong gradients separating the Scotian Shelf from the Gulf of Maine. Information on the continuity of water property flow past Cape Sable is obscured as an artifact of the increased tidally driven mixing west of the Cape meridian. The spatial distribution of the tidal kinetic energy has been illustrated by Greenberg (1977).

b. Maine Surface Water. The MSW has salinities between 31.6-33.2‰. In the near-shore regions, local runoff may depress salinity values further. The runoff is not evenly distributed: ~35% discharges into the western portion of the Gulf from Cape Cod to the Penobscot River, ~62% into the region from the Penobscot to the St. John River, and the remainder (~3%) into the Bay of Fundy. The 1-17°C temperature range (Fig. 4) reflects the seasonal heating and cooling cycle. Greater near-shore variations exist (see Speirs, Graham, and Dow, 1976). Vertical *T-S* gradients in MSW are reduced in the regions of greater tidal mixing, producing for example, higher salinities and lower temperatures in northeastern portion of the Gulf.

c. Maine Intermediate Water. The MIW is a low salinity, temperature minimum water. The salinities are too low to be of offshore origin, and the water mass volume shows seasonal fluctuation, thus local coastal formation is suggested. During the winter the MIW characteristics converge with the MSW, but during the spring the two water masses diverge as the MSW freshens and warms. The MIW is the remnant water mass from the previous winter. It is not correspondingly destroyed during summer heating because the mixing processes associated with cooling extend deeper than do those associated with warming. The MIW core is found around 75 m with a depth range and volume dependent upon seasonal production.

d. Maine Bottom Water. The MBW is a warmer, higher salinity water than the MIW. It occupies the depths between the MIW and the bottom. By definition its water type is unaffected directly by air-sea interaction (i.e. by definition because the direct effects are absorbed by the MIW). The only offshore exposure occurs through

the Northeast Channel, where entry of SW is determined on the basis of density. Incoming water has a route controlled by the bathymetry: after entry over the sill it flows into Georges Basin and thence westward to the Wilkinson Basin or northward to the Jordan Basin. None of the interior depressions is sufficiently large in volume to permit significant accumulations of a denser (than MBW) water mass.

e. Georges Bank Water. The GBW has been designated a separate water mass on the basis of its water type homogeneity and on the basis of its distribution which commonly does not extend off the Bank. The position of GBW on the *T-S* diagram (Fig. 4) implies closer association with the interior Gulf of Maine waters than exterior. This is more clearly indicated by the salinities, which over an annual cycle remain remarkably constant at around 32.5‰. For comparison, the surface 50 m inside the Gulf has an average of 32.4‰, and that offshore has 33.7‰.

f. Slope Water. The water encountered exterior to the Gulf of Maine, particularly off the Northeast Channel region, is referred to as slope water. The description and definition of the water masses in this region is lacking. The existence of a shelf-slope water front and occasional intrusions of Gulf Stream water are similar to the better described slope water region of the Mid-Atlantic Bight (e.g. Wright and Parker, 1976). The southern penetration of the Labrador Slope Water (Gatien, 1976) creates similarities to the slope water off the Scotian Shelf, which is discussed for example, by McLellan (1957) and Lee (1970). Following Gatien's (1976) analysis, we have distinguished between the slope water dominated by water of Gulf Stream origin and that dominated by water of Labrador Current, calling them upper SW and lower SW, respectively (Figs. 3 and 4). For purposes of this paper, references to SW imply a subsurface source water to the Gulf.

3. Budget calculations

The exchanges between Gulf of Maine water masses can be estimated through salt budget calculations. Conservation of heat is assumed in the MBW in order to increase the number of equations. The calculations are made over the year extending from September 1965 to September 1966. The main sources of error arise from the two assumptions: that of seasonal consistency in transport and that of uniform mixing. Further error is introduced through the assumptions inherent in the averaging of the data and choice of spatial divisions. The averages were weighted by volume and the divisions are indicated in the budgets discussed below.

a. Role of the SSW. The SSW has been cited as contributing to the Gulf of Maine surface waters. The SSW has a lower mean salinity than the MSW and therefore acts to freshen the Gulf. If the SSW import is constrained to the surface layer (0-50 m), a disproportionate upward flux of MIW (50-120 m) is required to main-

tain a salt balance. This is demonstrated in the following transport (T) and salt balances:

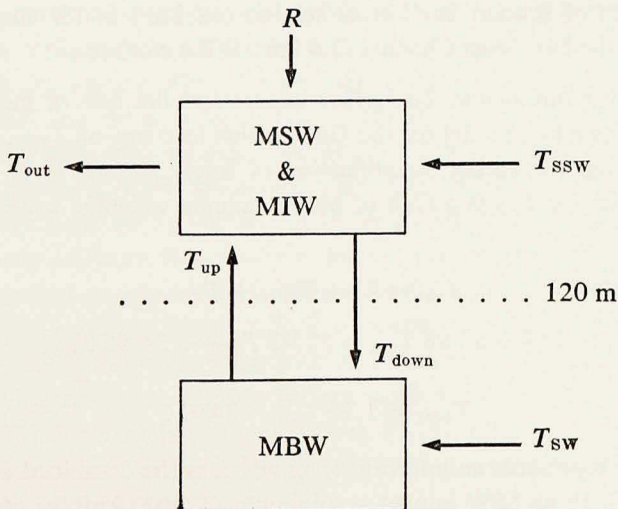
$$75 + T_{SSW} + T_{MIW} = T_{MSW} \quad (1)$$

$$31.79 T_{SSW} + 32.75 T_{MIW} = 32.39 T_{MSW} - 375 \quad (2)$$

where -375 is the annual change in salt for MSW. The runoff value (75) was based on a 30-year average river discharge (Meade, 1971) which has been corrected for the budget year by the variance observed (-19%) in the Penobscot River flow, and by the precipitation minus evaporation figures estimated from the Portland airport climatological data (U.S. Weather Bureau). The remaining coefficients are the volume averaged salinities at 10 and 50 m for SSW and MSW and at 75 m for MIW. In this case, the specification that T_{SSW} be greater than zero requires that T_{MIW} exceed $5700 \text{ km}^3/\text{yr}$. This is a volume greater than that occupied by the MIW, between 50-120 m, i.e., 4400 km^3 . A loss of this magnitude to the surface layer seems unrealistic because MIW also must experience losses via export from the Gulf and through mixing with the MBW. Therefore we conclude that if the SSW has a net import to the Gulf it must occur over a deeper depth range than the surface layer.

b. Balance for the entire Gulf. If the SSW is allowed to input to the MIW and MSW, a more credible balance is obtained. Consider a two layer system as depicted in the diagram below. The upper layer, consisting of a combination of MSW and MIW, is freshened by runoff R and by SSW and salted by MBW; the lower layer, consisting of MBW, is freshened by a downward flux of MIW and salted by SW.

For the MBW, conservation of heat is imposed. The SW average value is taken from stations 19, 20, 21 at 200 m for the four cruises. The T_{down} is taken to have



MIW (75 m) properties, and the T_{up} is taken to have the MBW (150 m) properties. The T_{out} salinity value is a volume weighted salinity average of the top 120 m. The SSW value was derived from a volume average of stations 13 through 18. The time derivatives are volume averages over their respective depths for the September 1965 to September 1966 period. $\Delta S/\Delta t$ for the upper and lower layers are -294 and 177 , respectively; and $\Delta T/\Delta t$ is 2544 in the lower layer.

The balance equations for the upper layer are:

$$T_{SSW} + T_{up} + 75 = T_{out} + T_{down} \quad (3)$$

$$-294 + 32.59 T_{out} + 32.75 T_{down} = 32.02 T_{SSW} + 33.62 T_{up} \quad (4)$$

and for the lower level:

$$T_{SW} + T_{down} = T_{up} \quad (5)$$

$$177 + 33.62 T_{up} = 34.66 T_{SW} + 32.75 T_{down} \quad (6)$$

$$2544 + 5.15 T_{up} = 6.79 T_{SW} + 4.57 T_{down} \quad (7)$$

Solution of this set of equations gives the following values:

$$T_{SW} = 2600 \text{ km}^3/\text{yr} \quad (80 \times 10^3 \text{ m}^3/\text{sec})$$

$$T_{down} = 2900 \text{ km}^3/\text{yr} \quad (90 \times 10^3 \text{ m}^3/\text{sec})$$

$$T_{up} = 5400 \text{ km}^3/\text{yr} \quad (170 \times 10^3 \text{ m}^3/\text{sec})$$

$$T_{out} = 7900 \text{ km}^3/\text{yr} \quad (250 \times 10^3 \text{ m}^3/\text{sec})$$

$$T_{SSW} = 5200 \text{ km}^3/\text{yr} \quad (170 \times 10^3 \text{ m}^3/\text{sec})$$

These values give a flushing time of 1.7 years for the MBW. The mean flow through the upper 120 m of Scotian Shelf cross section (12 km^2) is $1.4 \text{ cm}/\text{sec}$; and that below 120 m of the Northeast Channel (3.4 km^2) is $2.4 \text{ cm}/\text{sec}$.

c. Minimum SW requirement. To further understand the role of these two inputs, we consider a single box model for the Gulf, which in terms of T_{SSW} , represents the opposite case from the earlier simplification of solely surface layer entry. In this model, the salinity for T_{out} is a Gulf of Maine volume weighted average. The equations

$$T_{out} = 75 + T_{SSW} + T_{SW} \quad (8)$$

$$-117 + 32.98 T_{out} = 32.02 T_{SSW} + 34.66 T_{SW} \quad (9)$$

give

$$T_{SSW} = 1.75 T_{SW} - 2450. \quad (10)$$

The 2450 figure represents an intercept term which is the combined effect of R and $\Delta S/\Delta t$ (-117). With no SSW import, a minimum of $1400 \text{ km}^3/\text{yr}$ of SW would be

required. This may be contrasted with the 5700 km³/yr of MIW needed for the same purpose. After the minimum SW requirement, every two parts of SSW are approximately compensated for by one part of SW.

d. Budget discussion. The results of these budgets are sensitive to error in the temperature and salinity values. We feel that the slope water values become the most critical error source because of the small sample population available for their definition. These values should be selected from waters outside the channel, as opposed to in the channel, because much of the inter-layer exchange occurs in the channel itself (Hopkins, 1978). In the Colton *et al.* (1968) data, there are only three stations in the immediate vicinity of the Northeast Channel mouth. The particular slope region at the Northeast Channel mouth often has little water mass continuity shoreward of the shelf-slope front, that is between Browns and Georges Banks. As an example of the sensitivity, a 0.22‰ SW salinity change or a 0.15°C SW temperature change causes a 15% variation in the SW transport value.

The way the Gulf of Maine budget (Section b) has been formulated, T_{SW} is not a direct function of T_{SSW} , whereas the T_{SSW} depends directly on the T_{SW} . This is not strictly true. The T_{SW} is thermohaline driven whereas the T_{SSW} may be otherwise forced, as by windstress. Inequalities in the SSW salt and heat fluxes are compensated over short time scales by the time derivative terms of the balance equations, and over long time scales by differential salt and heat fluxes of the SW.

Brown and Beardsley's (1978) model of the Gulf of Maine is similar to the minimum SW requirement discussed in section c (Eqs. 8, 9, and 10). In order to determine the SW input they assumed a predetermined T_{SSW} value, the transport through the Scotian shelf cross section at Halifax. The requirement that all of the SSW passes through the Gulf of Maine gives a higher range of transport values than those determined in the present study where the SSW input is required only to satisfy the salt requirement in the upper (<120 m) layers.

The seasonal T - S cycling (Fig. 6) shows the salting to occur gradually from late spring to summer and through fall; whereas the freshening occurs more suddenly during the winter and early spring. The March MIW seasonal salinity minimum preceded the May-June MSW minimum. This suggests that the MIW minimum is not caused by the local spring runoff, but by an earlier maximum in the SSW contribution. There is evidence that the SSW import occurs in large intrusions during discrete winter events as opposed to a continuous flow over the year. The Jan.-Feb. 1969 data of Hayes (1975) shows a SSW intrusion where a large tongue of SSW penetrates westward through the Cape Sable to Browns Bank section into the eastern portion of the Gulf of Maine. Sudden surface salinity drops have been reported by Pawlowski (1977), for example dropping from 33.5‰ to 32.5‰ from February to March 1977. The lack of vertical density structure in winter facilitates SSW entry into the Gulf and into the deeper MIW.

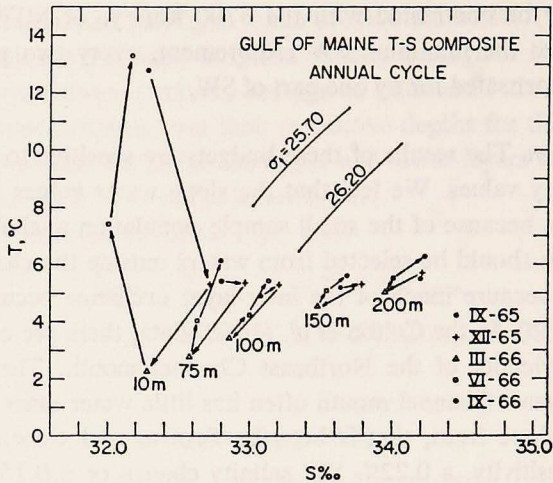


Figure 6. The cycling of the composite T - S values from all the Gulf of Maine stations through the data year September 1965 to September 1966.

There must also exist dynamic considerations that selectively effect the SW entry. The degree to which the internal thermohaline requirements determine the type of slope water available for entry cannot be determined explicitly from this data set apart from the constraint that $\rho_{SW} > \rho_{MBW}$. We note that during the stratified season, the lower layer over the sill is nearly isopycnal (from Stations 19 and 20 to Stations 29 and 30). During the unstratified season, the lower layer water is less dense inside the sill. The opposite is true inside the basin, as we note in the next section, i.e. the internal pressure gradient in the MBW is weakest in December and strongest in September. We suggest that SW entry is blocked during the unstratified season by adverse barotropic pressure gradients (a surplus of water inside the basin) and SW entry is maximal during the end of the stratified season when the internal baroclinic pressure gradient predominates. Thus the winter SSW intrusions and spring runoff maximums require a thermohaline adjustment manifested by a SW import during the stratified season.

4. The disposition of the MIW

The T - S properties of the upper layer (MSW & MIW) generally are not conserved from year to year, even though the residence time for this layer may be more than a year. The T - S properties of the MSW are altered seasonally and those of the MIW, annually. The water body defined by T - S properties has a shorter time scale than defined by volume. The MSW properties are a continuous function of surface exchange with the atmosphere; whereas those of the MIW are so for only several

Table 2. Maine Intermediate Water envelopes and volumes.

Date	Mean		Range		MIW Volume km ³
	Temp. °C	Sal. ‰	Temp. °C	Sal. ‰	
May '65	3.20	32.44	2.2-4.2	31.97-32.91	5800
Sept. '65	3.20	32.44	2.2-4.2	31.97-32.91	1200
May '66	3.96	32.67	3.1-4.9	32.01-33.23	5500
Sept. '66	3.96	32.67	3.1-4.9	32.01-33.23	1500
May '70	4.99	32.57	3.6-6.3	31.53-33.61	6500

months of the year. During the remainder of the year, the MIW properties are only a function of its mixing exposure to the layers above and below it. Additional information on the disposition of the MIW can be obtained by taking advantage of this fact.

We consider two sources of MIW loss: export and mixing. If the MIW is arbitrarily defined as a fixed water type and the volume of this is estimated, then reductions in this volume with time during the conservative portion of its cycle imply a loss of MIW. A MIW export from the Gulf of Maine will reduce the volume of the MIW layer. Mixing of the MIW with adjacent layers will cause its water type to drift.

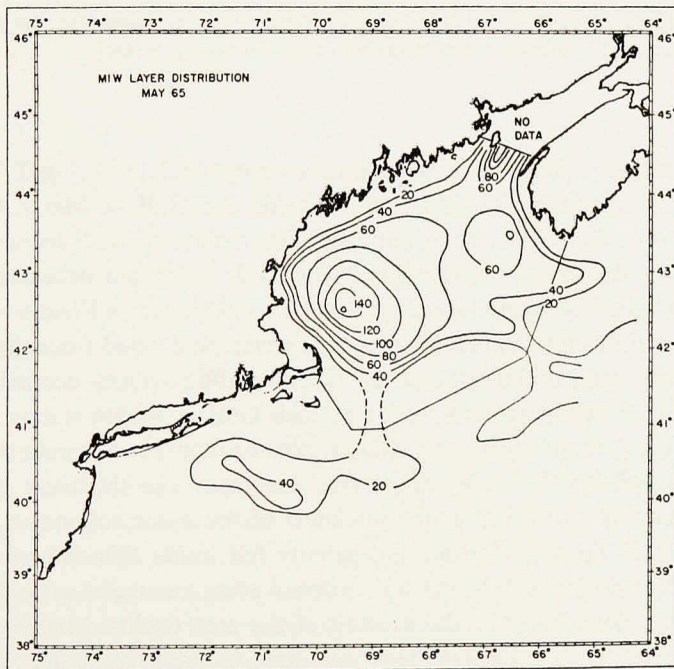


Figure 7. The distribution of the MIW layer, May-June 1965, as defined by the $T-S$ envelope, 2.2-4.2°C and 31.97-32.91‰. The contours represent the layer thickness in meters.

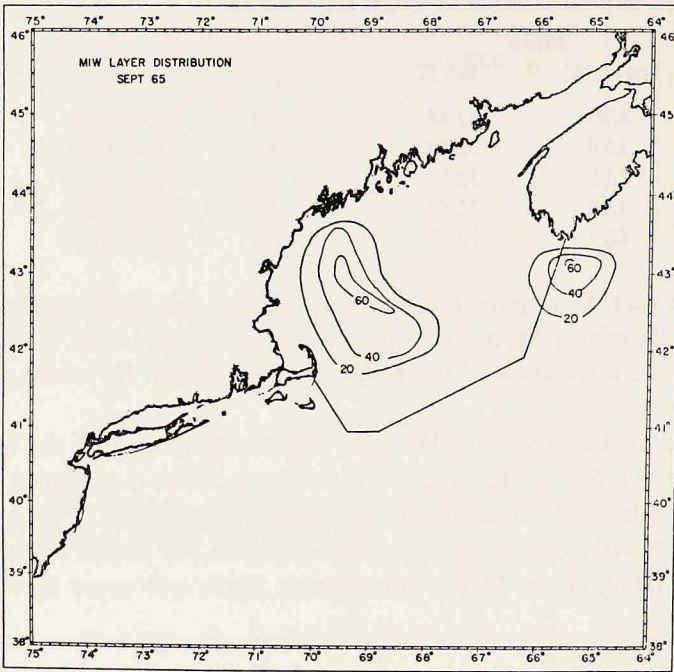


Figure 8. The distribution of the MIW layer, September 1965, as defined by the previous May T - S characteristics. The contours represent the layer thickness in meters.

a. MIW volume loss. Seasonal MIW volumes were calculated using T - S limits derived from the May-June T - S distributions inside the Gulf of Maine to illustrate the distribution of the MIW at a given time. When the spring distribution is compared with the fall distribution, the MIW volume deterioration over the summer is illustrated. The Gulf of Maine boundary was taken as shown in Figure 1. The MIW volumes were estimated from a T - S water type envelope defined from the late spring data. The temperature minimum and the corresponding salinity occurring between the 40 and 150 m depths were recorded at each Gulf of Maine station. These T - S values were averaged and their mean values, plus or minus two standard deviations, were taken as defining the MIW water type envelope. The thickness of the MIW layer at each station was taken as the thickness of the water column at that station within which both the temperature and salinity fell inside this T - S envelope. The values were plotted, contoured, and the enclosed areas measured with a planimeter. The volume was determined as the product of the area enclosed between two contour lines and the mean thickness. This was done for both May and September of 1965 and 1966 (Colton *et al.*, 1968) and for May of 1970 (Hayes, 1975). Table 2 gives the temperature and salinity means, ranges, and the calculated MIW volumes.

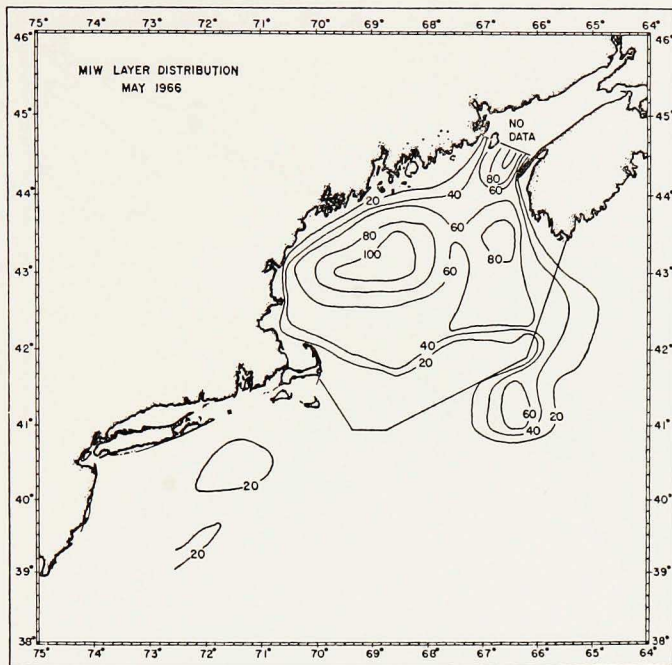


Figure 9. The distribution of the MIW layer, May-June 1966, as defined by the T - S envelope, 3.1-4.9°C and 32.01-33.23‰. The contours represent the layer thickness in meters.

The May 1965 distribution of MIW shows the thickest portion (> 160 m) centered over Wilkinson Basin (Fig. 7). Water type continuity exists through Northeast Channel onto the southeast flank of Georges Bank and to the northeast along the slope. A short tongue of MIW extends onto the Scotian Shelf north of Browns Bank. The SSW at this time had MIW-type temperatures and salinities but generally not occurring together at the same depth. The possibility of continuity through the Great South Channel exists and is shown with dotted lines. The central channel was not sampled, but the MIW was found well above the sill depth to the north and south of it. By September 1965, the MIW volume had diminished to 1/5 of its May volume, (Fig. 8). The major portion remained over Wilkinson Basin. A slug of MIW water type is centered just north of Browns Bank on the Scotian shelf where the tongue of the May distribution was found. This slug was not included in the September volume estimate as all but a small portion is outside the Gulf boundary.

In May 1966, the MIW layer was slightly less in volume than that of the preceding spring, but more evenly distributed in terms of thickness throughout the Gulf, and the center of maximum thickness was located north of Wilkinson Basin, (Fig. 9). As was the case in 1965, water type continuity is shown through Northeast

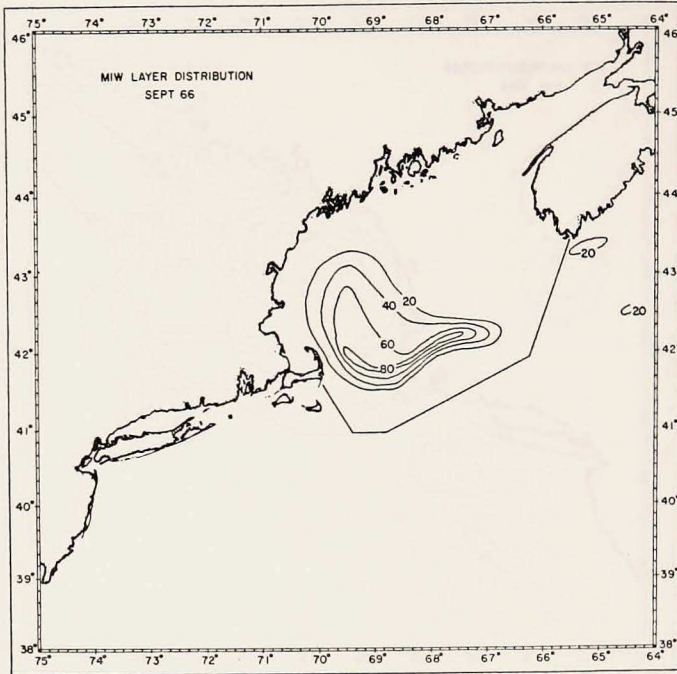


Figure 10. The distribution of the MIW layer, September 1966, as defined by the previous May *T-S* characteristics. The contours represent the layer thickness in meters.

Channel around the tip of Georges Bank and westward along the southeast flank of the bank. No water type continuity is discernible through Great South Channel although some MIW water type was found south of Long Island. By September 1966, the MIW volume within the Gulf was diminished to approximately $\frac{1}{4}$ the spring volume, and was centered around Wilkinson Basin (Fig. 10). No continuity of water type was found through either channel, although the distribution is strongly skewed toward the Northeast Channel.

To compare with a warmer year, the MIW volume distribution is shown for May 1970 (Fig. 11), calculated from Hayes (1975). The estimated volume turned out to be greater than that of the cooler years of 1965 and 1966, because of the greater *T-S* variability in the MIW. MIW water type continuity extends through Northeast Channel as was the case in the cooler years, but instead of skirting the northeast tip of Georges Bank, the water type extends eastward over the Scotian shelf. The situation south of Great South Channel is similar to 1965, MIW water type is present along the outer shelf from Great South Channel to at least Long Island, but due to the station locations, continuity of water type through the channel cannot be proven.

The situation on the south slope of Georges Bank is illustrated (Fig. 12) in greater

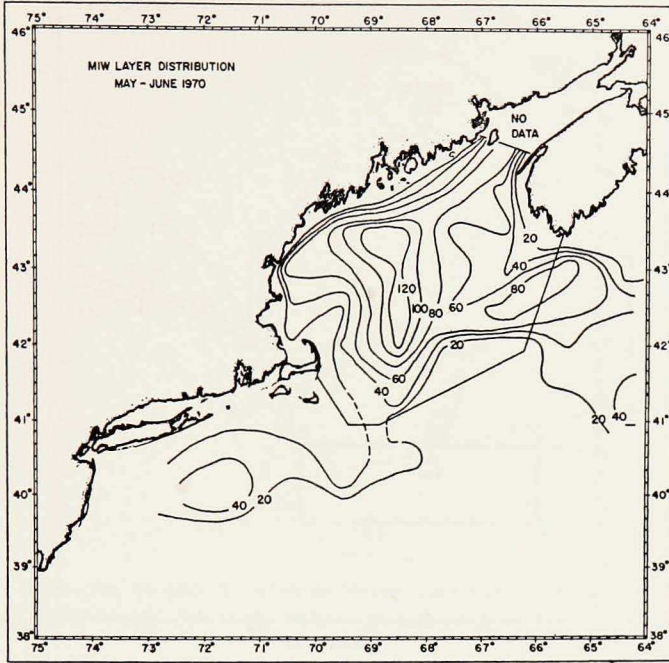


Figure 11. The distribution of the MIW layer, May-June 1970, as defined by the T - S envelope, 3.6-6.3°C and 31.53-33.61‰. The contours represent the layer thickness in meters.

detail to explore the possibility of MIW exiting around the outside of GB between stations. Station 39 had a water type at 30 and 40 m close to that of the MIW. Comparison with Station 38 suggests that MIW was not transported over Georges Bank. The farther offshore stations of 40 and 41 show some influence of mixing with a cold, low salinity water mass; whether it is of MIW or of SSW origin is not clear. The possibility of a thin band of MIW between Stations 39 and 40 is not excluded, but a more likely possibility is that the water type of the source MIW (or SSW) has been modified by mixing while travelling in a narrow band parallel to the Georges Bank outer slope.

Outside the Gulf of Maine, there is an uncertainty in identifying the MIW because of the potential for water type coincidence with the SSW and winter New England shelf water. It is beyond the scope of this work to discuss the relative volumes of these water masses exterior to the Gulf of Maine. We wish, however, to demonstrate that an appreciable volume of MIW is exported. The budget calculations showed that export from the upper layers must occur. In the next section the relative losses between mixing and export within the MIW, and the relative export between the MSW and MIW will be approximated. Before doing so, we would indicate why the export of MIW is preferred over MSW.

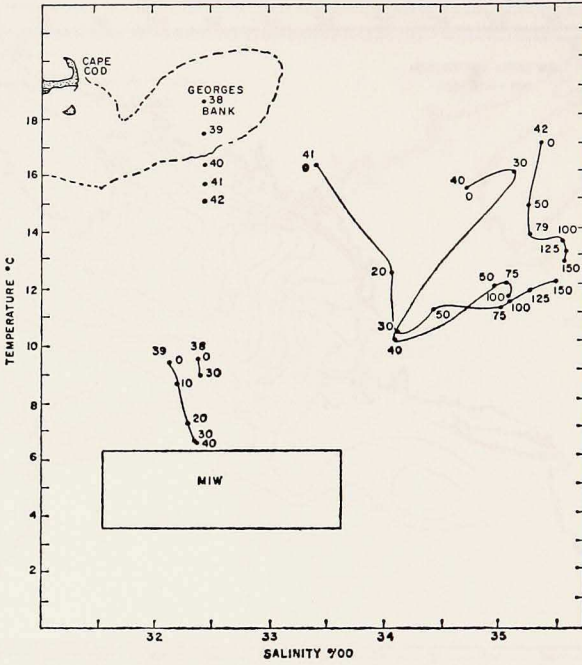


Figure 12. The location of the MIW envelope on a T-S diagram compared with Georges Bank stations, 38-42. The station locations are shown in upper left of diagram, the station numbers are placed at the start of each T-S curve, and the depths are labelled on each curve. Data is from Hayes (1975).

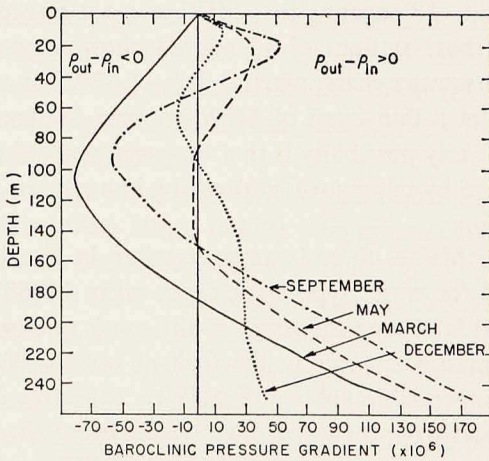


Figure 13. The baroclinic pressure gradient (cm/sec²) between stations 30 (Northeast Channel) and 65 (Wilkinson Basin) during data year December 1965 to September 1966. For values to the left of zero, the density inside is greater than that over the sill, and vice versa.

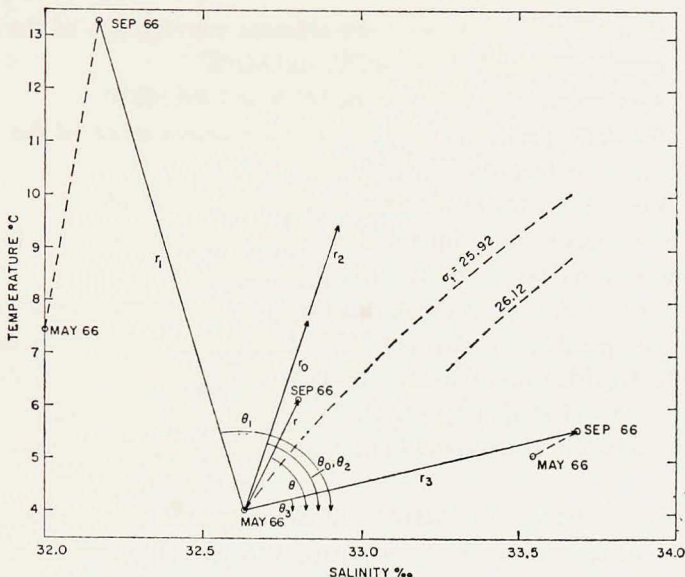


Figure 14. A T - S vector diagram for Gulf of Maine composite values of the MSW (left), MIW (center), and MBW (right). The vector notation is defined in the text.

The Gulf of Maine has been described earlier as a three layered basin except for the winter season when it was two layered. During the stratified seasons, the surface and bottom layers have less dense water than is found at comparable depths outside. The middle layer is more dense, and throughout the year the baroclinic horizontal density gradient has a minimum approximately at the depth of the MIW core. Figure 13 gives an example of the values of the integrated horizontal density gradient between a sill station (30) and an interior station (65). Export driven by internal pressure gradients is preferred at the depth of the MIW layer, and is enhanced with barotropic pressure compensation. That is, an accumulation of water inside the basin would move the zero line in Figure 13 to the right. In a three dimensional sense, this internal pressure field would force the MIW to accumulate and to exit along the northern boundary of Georges Bank.

b. T-S Drift. Another method of investigating the disposition of the MIW can be derived from an analysis of the seasonal change of the MIW water type. Vectors are constructed on a T - S plane corresponding to water type displacements. The displacement between successive observations is referred to as a T - S drift. The following analysis treats the MIW T - S drift between the May 1966 and September 1966 observation periods of Colton *et al.* (1968). The various T - S vectors are identified in Figure 14 as follows:

r, θ the seasonal drift of the MIW

- r_0, θ_0 the drift associated with the ultimate convergence of the MIW to an equal mixture of MIW, MSW, and MBW
- r_1, θ_1 the displacement between the MIW and the MSW
- r_2, θ_2 the drift associated with the ultimate convergence of the MIW to an equal mixture of MSW and MBW
- r_3, θ_3 the displacement between the MIW and the MBW

The salinity values were scaled by a factor of six to numerically weight them more evenly, with respect to density, to those of temperature.

The T - S values at the 75 m depth are taken to be representative of the MIW layer. It has been pointed out that the MIW core depth varied geographically and seasonally. The resulting uncertainties were less substantial in the Gulf-wide averages than at individual station locations. The MSW and MBW values were taken to be represented by the 10 m and 150 m data values. Again the type of uncertainty is obvious.

The observed T - S drifts of the MIW (r, θ) are compared with the two hypothetical drift situations, namely mixing (r_0, θ_0) and export (r_2, θ_2). The comparisons are made in the sense of the component of \vec{r} along either \vec{r}_0 or \vec{r}_2 . The values of $\frac{\vec{r} \cdot \vec{r}_0}{|\vec{r}_0|^2}$ indicate the relative degree to which the MIW T - S drift compares with a uniform mixture of the three water types: May MIW and September MSW and MBW. These values are interpreted as indicating the loss of MIW by mixing. The values of $\frac{\vec{r} \cdot \vec{r}_2}{|\vec{r}_2|^2}$ indicate the relative degree to which the MIW T - S drift compares with the extreme case in which the May MIW layer was completely removed such that by September the water at the 75 m depth is strictly a mixture of September MSW and MBW. These values are interpreted as indicating the amount of local MIW export.

There are a number of points that are relevant to the use of this method. It is assumed that the ultimate MIW mixture could not have been caused by the local advection of any external water mass, nor by any nonconservative process. This is not a restrictive constraint. There is no external water mass in the direction of MIW drift; and 75 m is below the depth of direct buoyancy addition as would occur by freshening or atmospheric heating.

Local advection within the MIW layer, import or export, will produce T - S displacements approximately parallel to the MIW drift and will be reflected in the values of $\frac{\vec{r} \cdot \vec{r}_2}{|\vec{r}_2|^2}$. Deviations from the mean value of θ_2 are primarily due to misrepresentations of the 75 m depth as the core MIW. The use of September MSW and MBW end point values for \vec{r}_1 and \vec{r}_3 effectively puts an upper bound on the magnitude of r_2 . Note that any end point values chosen between May and September for these vectors would not change θ_2 but only the magnitude of r_2 .

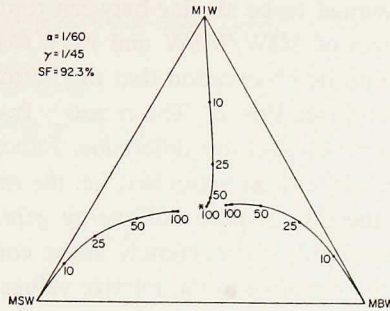


Figure 15. A water type phase diagram indicating the water type drift toward a complete mixture. The numbers indicate the sequential number of mixing events. The computation was based on $\alpha = 1/60$ volume exchange between MSW and MIW and on $\gamma = 1/45$ volume exchange between MBW and MIW per mixing event. The shrinkage factor (SF) is the areal decrease in the water type triangle per mixing event.

To discuss the T - S drift due to mixing, we consider the three layered system. Each layer is treated as homogeneous. The mixing between layers is assumed to be the result of repeated incremental volume exchanges or mixing events. The water type values for each layer can be expressed as a function of the initial values and a transition matrix, thus

$$\begin{pmatrix} \text{MSW}_n \\ \text{MIW}_n \\ \text{MBW}_n \end{pmatrix} = \begin{pmatrix} 1-\alpha & \alpha & 0 \\ \alpha & 1-\alpha-\gamma & \gamma \\ 0 & \gamma & 1-\gamma \end{pmatrix}^n \begin{pmatrix} \text{MSW}_0 \\ \text{MIW}_0 \\ \text{MBW}_0 \end{pmatrix}$$

where n is the number of mixing events and α and γ are the volume fractions mixed between the MIW/MSW and MIW/MBW, respectively. This represents a discrete time Markov chain process. The transition matrix is doubly stochastic. It has the property that for n sufficiently large the mixture approaches a stationary distribution, which is the mixture composed of one third (by volume) contributions from each layer. The convergence to the stationary distribution is more rapid for larger volume fractions, but in the limit is independent of the relative magnitude for α and γ , provided $\alpha, \gamma > 0$ and $\alpha + \gamma < 1$. The product of the eigenvalues of the transition matrix gives a shrinkage factor which indicates the reduction of area enclosed by the three water types of the phase diagram (Fig. 15) per mixing event, n . As n increases, the state of the mixture is increasingly independent of previous states.

The convergence of the middle layer is greater than three times more rapid than that for the adjacent layers. Furthermore, for reasonably close values of α and γ , convergence for the middle layer is nearly linear. These two points are demonstrated in Figure 15 in which α is taken as slightly smaller than γ . The assumption that they are approximately equal is derived from the observation that the work required for mixing comes primarily from the dissipation of the barotropic tides by bottom fric-

tion. The dissipation is assumed to be similar between the two layers on the basis that the interfacial exposures of MIW/MSW and MIW/MBW to the bottom are equivalent. This follows from the observation that the bottom area changes linearly through the MIW depth band (see Fig. 2). The α and γ fractions are assumed also to vary inversely as the interfacial density difference. Effectively, their dependence is similar to an inverse flux Richardson's Number, i.e. the ratio of the rate of turbulent energy production to the rate of potential energy gain. The advantage in this application is that the fairly rapid, approximately linear convergence of the middle layer to its mixed value is not sensitive to the relative values of α and γ nor to their absolute values.

Figures 14 and 15 will serve to illustrate another point. The rate of convergence of the MIW is enhanced further relative to that of the MSW and MBW; because the MIW drift is assumed to be only due to mixing (local export excluded), whereas that of the MSW and MBW are additionally due to external water mass input and nonconservative processes (MSW). The T - S displacement of the MSW between May and September (Fig. 14) is the vector sum of a displacement due to air-sea interaction exchanges of heat and water vapor, to runoff, to SSW inflow, and to the mixing drift. The first and last of these are assumed to be the most significant during this period (stratified); e.g. the May-September displacement would extend to warmer temperatures and fresher salinities without the influence of the drift caused by MIW and MBW mixtures. Of the three layers, only the MIW will display a T - S drift track similar to that shown in Figure 15. Use of the September end point values for \vec{r}_1 and \vec{r}_3 provides an upper bound for the convergent mixture, \vec{r}_0 . The lower bound for \vec{r}_0 is zero. Negative values are not possible since the mixing process is irreversible. The direction of the mixing drift, θ_0 , is insensitive to the end points of \vec{r}_1 and \vec{r}_3 , slightly sensitive to the values of α and γ , and most sensitive to unrepresentative sampling of the local MIW water type.

The α and γ values of Figure 15 are purely illustrative. However, they may be considered as estimates of the magnitude of volume exchange that could occur per tidal cycle. Note that the barotropic tide-bottom friction mechanism has a geographic bias for those areas where the layer interfaces intersect the bottom, such that α and γ are in these locations larger. Away from these areas of intersection, interfacial mixing is possible but is minimized by the opposing effects of shear and stability on the mixed volume fractions. Local variations in the MIW drift are evident in the results, e.g. by local deviations of θ_0 from the mean value of θ_0 . This is considered as evidence that α and γ do vary geographically and that the time scale for vertical mixing is shorter than that for horizontal dispersion. Furthermore, the assumption that α and γ represent discrete volume exchanges is not significant with respect to the convergence of the stochastic process, i.e. a similar convergence is obtained with continuous (in time) exchange parameters.

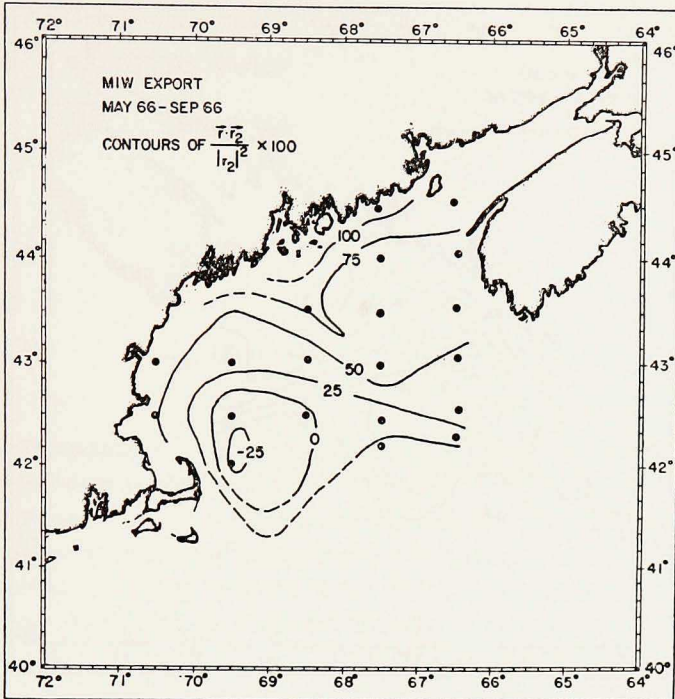


Figure 16. The distribution of the MIW layer export, defined as the component of \vec{r} along \vec{r}_2 , and expressed in percent.

The two processes of local vertical mixing and local export are assumed to be independent, the former involving mesoscale conversion of kinetic energy to potential energy and the latter involving large scale (greater than station grid) horizontal transport. With respect to this analysis, this assumption means that \vec{r} is compared to \vec{r}_0 separately from \vec{r}_2 and vice versa. The degree of independence is based on scale separation. This is not entirely valid, for example, a MIW export effectively increases α and γ . Although these processes are relatively independent, their effects are relatively correlated. For example, maximums in transport and mixing tend to occur around the basin periphery.

The contours of $\frac{\vec{r} \cdot \vec{r}_2}{|\vec{r}_2|^2}$ (Fig. 16) $\frac{\vec{r} \cdot \vec{r}_0}{|\vec{r}_0|^2}$ (Fig. 17) demonstrate similar distributions, that is, regions of large export have large mixing losses and those of smaller export, or even import, also have small mixing losses. The most pronounced feature is centered over Wilkinson Basin. Here the T - S drift components at several stations were negative, which is interpreted as indicating that local import of MIW dominated at the 75 m depth to the extent of completely suppressing any effects of mix-

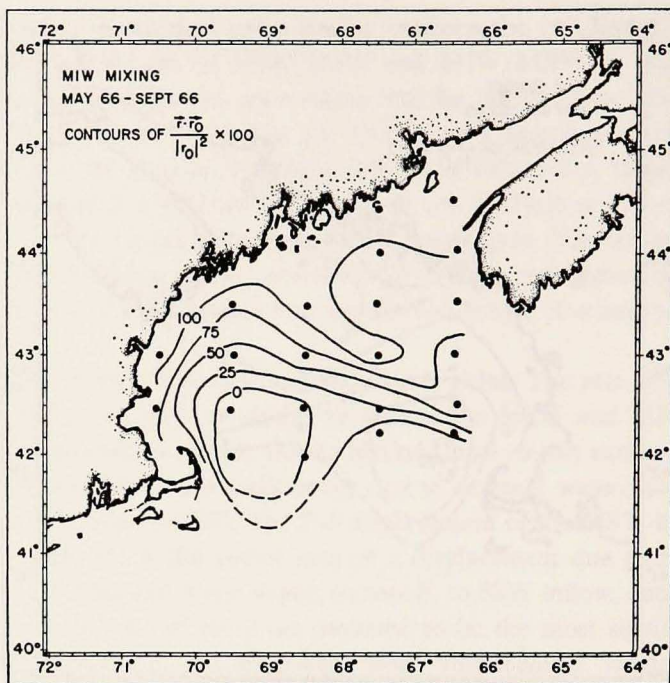


Figure 17. The distribution of the MIW mixing, defined as the component of \vec{r} along \vec{r}_0 , and expressed in percent.

ture with MSW and MBW. Note that a portion of the negative value may be attributed to sampling error, e.g. that the center MIW core was not sampled in May at 75 m but was in September.

The contours are closed (dashed) around the southern sector of Wilkinson Basin where no data were available. A middle layer convergence is dynamically compatible with a surface layer cyclonic gyre over the Wilkinson Basin. The region of low mixing loss and small export extends east from Wilkinson Basin toward Northeast Channel. Again this suggests preferential MIW accumulation in this band.

A relative maximum in both distributions extends southeast over the bathymetric ridge separating Wilkinson and Jordan Basins. It constitutes a significant intrusion of maximal values into the Gulf of Maine interior which otherwise are confined to the nearshore stations. Consequently, the Jordan Basin region is defined by relative minimum values, although its values are still significantly in excess of the Gulf of Maine average. The ridge demonstrates the bathymetric control for both processes. In the case of MIW export, the region over this ridge represents a middle layer divergence; and in the case of mixing loss, larger interlayer exchanges. In contrast to Bigelow's (1927) single gulf-wide gyre, these distributions imply a more compli-

Table 3. MIW *T-S* Drift Vector Statistics.

1. Vector	Vector Average	2. Component	% Magnitude
r, θ	2.4, 64°	$\vec{r} \cdot \vec{r}_0 / r_0 ^2$	63%
r_0, θ_0	3.8, 72°	$\vec{r} \cdot \vec{r}_1 / r_1 ^2$	18%
r_1, θ_1	9.6, 107°	$\vec{r} \cdot \vec{r}_2 / r_2 ^2$	42%
r_2, θ_2	5.7, 72°	$\vec{r} \cdot \vec{r}_3 / r_3 ^2$	24%
r_3, θ_3	6.5, 14°		

cated system composed of a strong Wilkinson Basin gyre and a less well defined secondary system over Jordan Basin.

We now consider the Gulf of Maine average values of the drift vectors to make quantitative assessments of Gulf-wide values for mixing and export. The average values are given in Table 3 as computed from the 22 Gulf stations used.

The direction of the drift, θ , indicates the mixing preference of the MIW. The average value of $\theta = 64^\circ$ fell toward a MBW mixture from the theoretical mixtures of $\theta_0 = 72^\circ$. Taken individually, the central stations favored MBW mixtures while the perimenter stations favored MSW mixtures. This follows since the kinetic energy dissipation associated with the intersection of the MSW/MIW interface and the bottom is shoreward of the MIW/MBW interface intersection. The directional drift is not entirely linear between an initial and the final *T-S* mixture. The observed drifts will manifest some nonlinearity (e.g. Fig. 15) according to the discrepancy between α and γ . For the mean values illustrated in Figure 14 the isopycnal condition ($\theta \cong 46^\circ$) falls on the MBW side of the ultimate mixture, so that the lesser stability between the MIW and MBW is reflected in the general preference for MBW mixture.

c. Comparison of results. The Gulf-wide averages from the *T-S* drift analysis and the *T-S* volume analysis can be used for comparison with the results from the budget calculations. If the mixing and export losses are normalized to 100%, they become 60% and 40%, respectively. In September 1966 there remained 1500 km³ of MIW within the *T-S* envelope (Table 2). If this envelope is superimposed on Figure 14, it includes 41% of the drift vector (\vec{r}). On this basis, we estimate a total of 3700 km³ for the seasonal *T-S* drift volume. In terms of volume, the mixing and export losses are 2200 and 1500 km³, respectively. For the mixing loss, we will make a comparison with the exchange of MIW to MBW. The mixing loss is first multiplied by a factor of 24/(18 + 24) from Table 3 to adjust for the preference for MBW mixing, and then multiplied by a factor of 1/2 to account for the net amount of MIW

lost to MBW. The result is 630 km^3 which can be compared with $T_{\text{down}} = 850 \text{ km}^3$, when the annual figure is interpolated to the May to September period. These values convert to a vertical mixing speed of $\sim 2 \times 10^{-4} \text{ cm/sec}$. The total upwards speed is doubled when the thermohaline circulation requirement is included.

We can not explicitly compare the export values, because the budget parameter T_{out} includes both MSW and MIW. However, if the results of the two analyses are expressed over an equivalent time period, a 5:3 preference for MIW over MSW export is indicated. Again, Figure 13 confirms this preference.

5. MIW formation

The uniqueness of the MIW might be in question unless it can be shown that the MIW can be produced locally via exposure to atmospheric buoyancy extraction, and that it is not the consequence of advection of a pre-formed water mass into the Gulf of Maine basin.

a. SSW advection. The primary candidate for advective input is the SSW. We have given evidence that the major portion of the SSW import occurs during the winter. The March 1966 mean values for the upper 50 m of the MIW and SSW were 2.31° and 32.3‰ vice 0.80° and 31.7‰ , respectively. Hence by the end of winter, the MIW was distinct from the SSW in water type and in geographic location. Without a SSW contribution, however, the winter water in the Gulf of Maine would have been saltier and would have formed a deeper layer. The fact that the SSW is cooler, and thereby corresponds to additional heat loss sustained by the surface convective layer, is relatively insignificant. If the entire SSW (5200 km^3) input entered during the winter with a temperature difference of 1.5°C , it would correspond to an additional loss of 68 ly dy^{-1} from the Gulf of Maine surface.

The advective heat loss term depends on the surface heat transport specific to an area and time; of all the terms of the heat budget, it is the most difficult to estimate independently. It is a much smaller percentage of the heat budget than the corresponding salt advection term is in the salt budget. To demonstrate this, consider a scaling of the advective term relative to the evaporative term in the heat and salt balance equations. If l_θ is a horizontal length of thermal change and l_s the corresponding length of salt change, then their relative importance can be scaled in the ratio,

$$\frac{l_s}{l_\theta} = \frac{L \cdot E}{C_p \cdot \theta \cdot (P - E)}$$

where L is the latent heat conversion, C_p the specific heat, P the precipitation, E the evaporation, and θ the temperature. The length scale for salt is effectively two orders of magnitude greater than for temperature. For example, in the Gulf of Maine the advective influence in the SSW input would be equivalent at 5 km and 500 km downstream for heat and salt, respectively. However, we have noted that the SSW

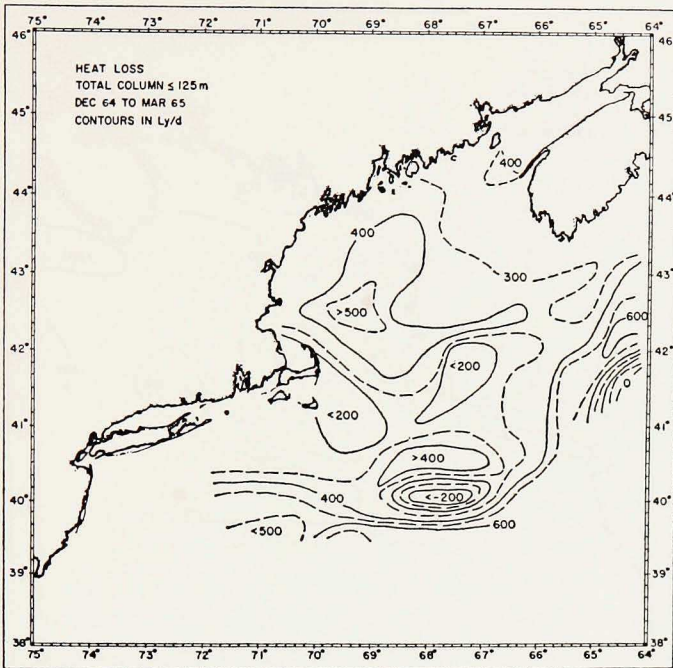


Figure 18. The observed heat loss in Ly/d from December 1964 to March 1965 of water columns to 125 m or the bottom.

is not restricted to surface entry. Consequently, the SSW can play a modifying role in the MIW formation by way of subsurface heat loss and general upper layer salinity depression.

b. Observed heat losses. In order to compare the estimate of local atmospheric buoyancy extraction with local observed water column heat losses, it is necessary to differentiate between a surface layer that is affected by air-sea heat exchange and a subsurface layer that is not. This surface (or convective) layer is itself difficult to determine unambiguously. Three figures are given to demonstrate the magnitude of the heat loss sustained during the winter 1965.

Figure 18 depicts the total heat loss of water columns to the bottom or to 125 m. The distribution is smooth in the Gulf of Maine with a local maximum over the Wilkinson Basin. In the slope region exaggerated variations are observed with a range of values in excess of 1100 ly d^{-1} . These are due to advective changes in the subsurface layers and geographic changes in the shelf-slope front.

Figure 19 is based on heat loss estimates using the depth of the March homogeneous layer as the depth of the convective layer. The water type variance permitted in determining the homogeneous layer was 0.6°C and 0.1‰ i.e. either causing $\sim 7 (10^{-5})$ change in density. The minimum values ($< 100 \text{ ly d}^{-1}$) were to the west,

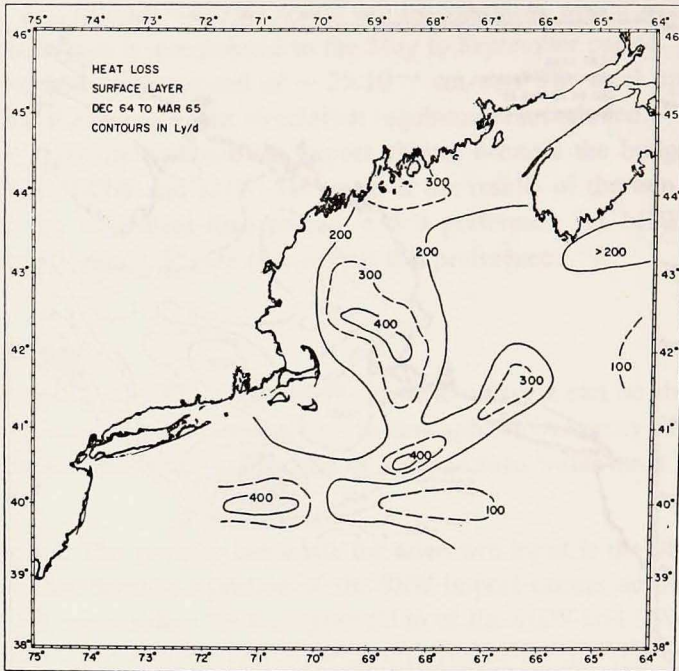


Figure 19. The observed heat loss Ly/d from December 1964 to March 1965 of the surface layer as defined by March homogeneous layer ($\Delta T \leq 0.6^\circ\text{C}$ or $\Delta S \leq 0.1\text{‰}$).

increasing rapidly eastward to a maximum (400 ly d^{-1}) over the Wilkinson Basin, and decreasing ($\sim 175 \text{ ly d}^{-1}$) in the eastern portions of the Gulf of Maine. The New England Shelf, Georges Bank, and Eastern Gulf of Maine/Scotian shelf areas had heat losses typically around 200 ly d^{-1} . Slightly higher values were observed in the northeastern portions of the Gulf. In the slope region, large variances were still present, with values ranging from 440 to -9 ly/day , presumably due to geographic variations in the surface manifestation of the shelf-slope front.

If the difference between the homogeneous layer and the upper 125 m is plotted (Fig. 20), the contribution of subsurface cooling is illustrated. Note that subsurface layer in this case varies in thickness. The values indicate the amount of subsurface (advective) cooling relative to surface (convective) cooling in the upper 125 m. The Georges Bank and New England shelf are relatively immune to subsurface advection of cooler waters, whereas the slope waters show considerable effect. The subsurface cooling inside the mouth of Northeast Channel could indicate the presence of a cooler water mass entering or leaving the Gulf. Its T - S properties suggest the latter. Within the Gulf of Maine, the low values of subsurface cooling over the Western Basin imply a surface convergence relative to those areas of higher subsurface heat loss. For example, the high values along the western shore may be ex-

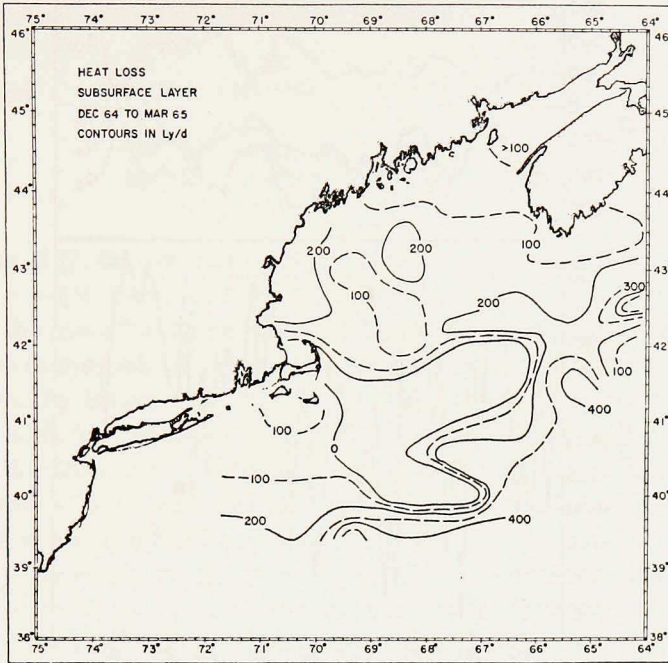


Figure 20. The observed heat loss Ly/d from December 1964 to March 1965 of the water columns below the March homogeneous layer depth and above 125 m or the bottom.

plained by subsurface import, or upwelling, of colder offshore (Wilkinson Basin) waters. The regional means for the observed heat losses and mixed layer depths are given in Table 4.

c. Potential for local production. We have seen that advective heat losses into the Gulf of Maine system are significant but not dominant. Atmospheric buoyancy

Table 4. Observed Heat Losses,* 12 December 1964 to 13 March 1965.

Region	Number of Stations	Depth (m) of Homo- geneous Layer	Heat Loss (Ly/d)		Difference (Ly/d)
			Homo- geneous Layer	Heat Loss (Ly/d) to 125m	
Gulf of Maine	26	56±23	231±92	362±96	131
Georges Bank	6	59±18	237±66	274±94	37
New England Shelf	7	46±15	204±44	233±86	29
Scotian Shelf	6	40±11	185±49	298±86	113
Slope	21	31±15	190±127	403±270	218

* Plus or minus one standard deviation.

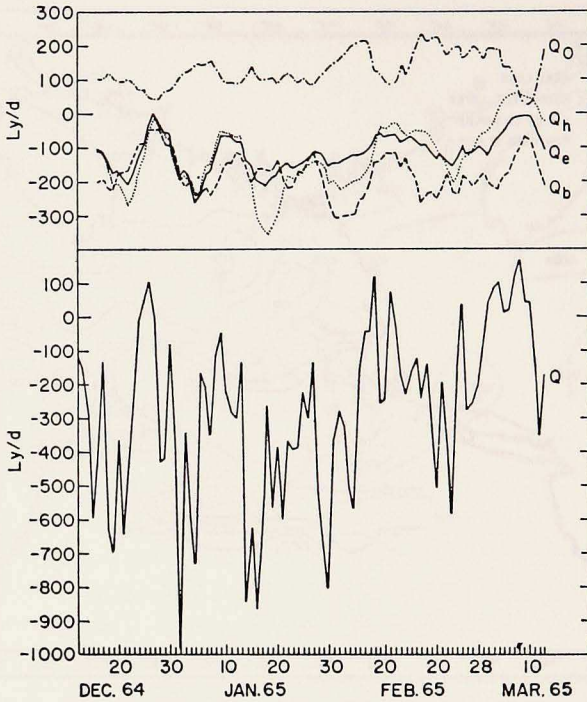


Figure 21. Five point running means of the daily heat flux terms (upper): Q_0 is the net incident radiation, Q_h is the sensible heat exchange, Q_e is the evaporative heat, and Q_b is the effective back radiation. In the lower portion is shown the corresponding daily total heat flux term for the winter 1965 period.

extraction processes must be reviewed as being the primary heat loss mechanism. Unfortunately, satisfactory confirmation is difficult due to certain constraints in computing heat and water vapor exchange and in extrapolating land based data offshore.

The geographic location of the Gulf of Maine enhances its exposure to continental air masses, as it is situated in the continental lee of the westerlies. The potential for atmospheric buoyancy extraction is favored during the cooling season. Westerly and northerly (offshore) winds prevail from October through March and average slightly stronger (4.9 m/s) than the prevailing southerly winds (4.4 m/s) of the warming season (U.S. Weather Bureau).

The primary cooling events rely on correlations between cold air temperatures, low humidities, cloudiness, and high wind speeds. They are difficult to extract from historical weather data, because of inaccurate empirical formulae and insufficient high frequency resolution. Estimations of the various heat loss terms for the period 12 December, 1964 to 13 March, 1965 are given in Table 5 and illustrated in Figure 21. The quantitative methods are explained in the Appendix. The large variability in the daily values is obvious from the standard deviation values and

Table 5. Mean Heat Losses (Ly/d), December 12, 1964-March 13, 1965.

	Q_i	Q_b	Q_e	Q_h	Q_r	Q
Mean \pm Standard Deviation	149 \pm 78	-181 \pm 106	-117 \pm 84	-124 \pm 127	-5 \pm 1	-278 \pm 254
Min.	+50	-382	-369	-548	-7	-980
Max.	324	-42	+47	+117	-3	116

from the plot of Q , the net heat exchange. The running mean of Q (not shown) is constant at ~ -350 Ly/d from mid-December until the first of March whence it increases to the mean for the period -280 Ly/d. This falls within range of the observed values in the Gulf of Maine. The net heat flux term has been estimated for another period by Brown and Beardsley (1978) from the Portland Lightship data to compare with their observed heat losses. They calculated a mean heat flux of -400 Ly/d for December 1974 with peaks in excess of -1000 Ly/d during five separate events. They observed heat losses of -250 and -125 Ly/d from two thermograph at 33m depth, 12 and 38 km offshore.

Four other curves are presented in Figure 21 to illustrate the trends in the net incident radiation Q_0 ($Q_i - Q_r$), evaporation Q_e , sensible heat Q_h , and effective back radiation Q_b . These are 5 point running averages of daily values. Q_h increased during the latter half of the period as air temperatures warmed; the Bowman's ratio decreased from 1.0 to -0.5 from the December values to the March values. Five cooling events occurred during the period with a periodicity of about 2 weeks. These range in characteristics from low humidities, clear skies, and high winds (evaporative events, e.g. 1-4 Jan.) to very cold and cloudy skies (sensible heat events, e.g. 16 Jan.). The combination of Q_0 and Q_b represents the net heat available and is a relatively smooth, low amplitude function. The variability is damped because of the inverse dependence on cloudiness; and for the winter period the two magnitudes approximately cancel. In this case, their sum trended from -46 Ly/d in December to 48 Ly/d in March.

It is the negative peaks in the Q_e and Q_h terms that principally cause the buoyancy extraction events. Both of these terms depend on small scale air-sea interfacial gradients, whereas the Q_0 and Q_b terms depend on larger scale conditions. In the case of the former, the accuracy of any extrapolation offshore is affected. Q_e and Q_h each may have different length scales. The sensible heat loss term depends primarily on the air-sea temperature difference, having in most cases a maximum at the coast. The importance of Q_h diminishes as the water columns lose heat through the cooling season (e.g. Fig. 21). Q_e is primarily a function of the water vapor difference. The fact that water vapor content itself is not a linear function of temperature can cause offshore maximums in the evaporative heat loss (Hopkins, 1976). Both of these terms can have secondary maximums associated with an offshore warm front.

The distance offshore in which the ocean manifests the effects of atmospheric

exchange defines an oceanic boundary layer which is uncoupled to the driving atmospheric boundary layer for reasons of specific heat and circulation. It is less complicated only perhaps because of its lower frequency response: in the atmosphere the temporal dependence is closely coupled to the wind direction as Bunker (1956) has shown, while in the coastal ocean high frequency changes are buffered by convective mechanisms leaving the weekly to seasonal frequencies predominant. An important difference is that in the ocean the major advective component has an along-shore bias which tends to compress the width of the oceanic boundary layer relative to that in the atmosphere. From airborne observations extending 150 km into the Gulf of Maine from Portland, Bunker (1956) found little change in air turbulence for cases of cold, offshore winds. The atmospheric horizontal boundary layer is complicated by strong advection seaward. In other cases, Bunker (1960 and 1972) has reported that the downstream persistence of vertically unstable air is extensive, on the order of 500 m for severe cases. Saunders (1977) reported that in terms of wind stress a maxima is found about 200 km offshore based on a statistical summary of ship wind reports. We expect the atmospheric length scale to be on the order of the Gulf of Maine dimensions, with the implication that severe exchange events would encompass the Gulf.

If Figure 19 is again consulted, a band of higher heat loss values approximately parallels the coast from the New England Shelf through the Gulf of Maine. This suggests an offshore heat loss maximum at ~ 150 km. The spur over Georges Bank is in part attributable to its shallow depths precluding heat flux up from below the convective layer. The localized maximum over Wilkinson Basin demonstrates the concentrating cooling effected by the local cyclonic circulation, reminiscent of the winter gyre off the Gulf of Lions (e.g. Hopkins, 1978). Caution should be used in extrapolating heat loss values inshore from the stations given, for example in Figure 19. An additional heat loss maximum can be effected by early winter, nearshore maxima in Q_h . These spacial and temporal changes in heat loss tend to smooth out with integration, so that the computed Portland value of 280 Ly/d might better be compared with the observed Gulf of Maine average of 230 Ly/d than with points more specific in space and time.

6. Summary

We expect the thermohaline dynamics as presented in this work to be representative but not necessarily typical for any given year. The system is not in steady state. Salt and heat contents are affected directly by annual and long term trends, such as the ~ 22 year periodicity indicated in the Colton (1968) paper, and indirectly by variations in the dynamics that control internal mixing and exterior water mass availability. Long term trends in heat and salt contents tend to conserve the potential energy of the basin and have periodicities prescribed by the basin's intrinsic

response to the combination of atmospheric, Scotian shelf, and slope water trends.

The Gulf of Maine can be considered as a three layered water mass system during all but the winter season when the upper two layers merge. The thermohaline circulation can be separated into a positive ($\rho_{in} < \rho_{out}$) circulation between the MIW and MBW layers; and a negative circulation between the MSW and MIW layers. The latter is less well defined and may reverse or become indistinct, as for example during winter. The result of these circulations is a net convergence in the MIW layer. The net upwelling from the MBW to the MIW was estimated at 2600 km³/yr (equal to the SW input). The amount mixed between these two layers was of the same magnitude, 2900 km³/yr from salt balance analysis and 2200 km³/yr from *T-S* drift analysis. The export of the upper two layers was estimated at 7900 km³/yr of which 5100 km³/yr was estimated to be MIW. The greatest mixing losses sustained by the MIW occurred in the northeastern portion where the dissipation of tidal energy is the greatest. The MIW appeared to collect over the Wilkinson Basin during the stratified season, to exit via the Great South Channel during early spring, and to exit via the Northeast Channel during spring and summer.

The Wilkinson Basin contains a surface cyclonic gyre. This is the primary circulation feature of the Gulf of Maine. It is more pronounced than the circulation over the Jordan Basin, where greater tidal mixing reduces the baroclinic structure. The amount of recirculation in the Wilkinson gyre was not estimated but the main exit for the surface layers appears to be eastward toward the Northeast Channel. The Wilkinson gyre receives surface and intermediate water along the Maine coast from the northeast during times of high alongshore coherence.

Both the SSW and the SW are input water masses. The SSW entry is incidental whereas the SW entry is necessary to the Gulf of Maine thermohaline circulation. Runoff alone required 1400 km³/yr of SW, and the SSW input required an additional 1200 km³/yr, which suggests an approximate equality between runoff and SSW in terms of freshwater input. It was demonstrated as unlikely that the SSW inputs only to the MSW on the basis that the MIW is too fresh; and it was suggested that the SSW input occurs mainly in discrete intrusions during winter when the horizontal and vertical density gradients are at a minimum.

The water over Georges Bank defines a distinct water mass by reason of its homogeneity and low seasonal variance in salinity. The mean salinity for the data period was 32.5‰ which excludes any more than ~10% contribution of offshore slope water. The most probable source water was MSW during late winter-early spring when MSW were less than 32.5‰ and no density gradients were present to inhibit an exchange.

Heat loss estimates derived from Portland airport data gave an average value of 280 Ly/d for the winter of 1965. This was higher than the loss (230 Ly/d) sustained by the water columns defined by the March homogeneous layer but less than the loss (360 Ly/d) of the 125 m water columns. The observed heat losses showed

significant offshore variations including a maximum in a band 150-200 km offshore; but these could not be directly attributable to offshore variations in heat flux because of the uncertainty generated by surface circulations. The SSW advective heat loss is limited to less than -70 Ly/d by the condition that all of the SSW input occur during winter. Even at this amount, the SSW input is not critical to dense water production because the negative buoyancy associated with the heat loss is offset by the positive buoyancy gained by its low salinity input. It is concluded that the production of the MIW is a local phenomenon characteristic of the Gulf of Maine.

Acknowledgments. The authors are grateful for the encouragement given them during the preparing of this manuscript by J. J. Walsh and C. S. Yentsch. We appreciate the helpful discussions with W. S. Brown and the computations made by C. D. Wirick. The research was supported by the Department of Energy under contract No. EY-76-C02-0016.

APPENDIX I. Heat Exchange Across the Air-Sea Interface

The following is a summary of the formulas and procedures used in estimating the daily heat exchange across the air-sea interface. For explanation of notation and units, see the end of this summary.

The daily heat exchange, Q , is represented by equation 1:

$$Q = Q_i - Q_r - Q_b - Q_o - Q_n \quad (1)$$

Q_i , the total incoming radiation from direct solar radiation, Q_s , plus diffuse sky radiation, Q_d , was not measured during the study period but the percent sunshine (s) was recorded. Daily insolation data were available for December 1970 to March 1971 and December 1971 to March 1972, and were used with the percent sunshine recorded at the Portland airport (U.S. Weather Bureau) to obtain a linear correlation between radiation data Q_i and percent of possible sunshine. Monthly regressions were computed from the data sets to account for the change in altitude of the sun and the increase in hours of sunlight. The major source of error in this calculation is that the radiation data was recorded at a site (Maine Yankee Atomic Power Plant) approximately 40 miles away from Portland airport where the hours of sunshine and cloud cover data were obtained. Both of these sites have the same general proximity to the ocean, but short term local conditions could be different at the two sites. The four regressions obtained by this method are:

$$\text{Dec } Q_i = 0.93(s) + 52.89 \quad r^2 = 0.70 \quad (2)$$

$$\text{Jan } Q_i = 1.20(s) + 50.21 \quad r^2 = 0.83 \quad (3)$$

$$\text{Feb } Q_i = 1.73(s) + 90.08 \quad r^2 = 0.78 \quad (4)$$

$$\text{Mar } Q_i = 2.54(s) + 70.10 \quad r^2 = 0.82 \quad (5)$$

The reflection back at the sea surface Q_r was determined by the equations reported by Burt (1953) and Neumann and Pierson (1966):

$$Q_r = rQ_i, \text{ where} \quad (6)$$

$$r = 0.066 \frac{Q_d}{Q_i} + 0.02 e^{-0.106h} \frac{Q_s}{Q_i}, \text{ and} \quad (7)$$

$$\frac{Q_d}{Q_i} = (e^{-0.074h} - 0.85) \cos(0.9C) + 1. \quad (8)$$

h = root mean square of the sun's maximum altitude (E_s) and

$$E_s = 25.5 \cos \frac{2\pi T}{365} + 47 \quad (9)$$

is used to calculate the sun's maximum altitude at Portland, Maine (44°N). T is the day of the year beginning with $T_{\text{Jan } 21} = 1$.

The effective back radiation Q_b was calculated using the formula by Shuleikin (1959) modified for cloud cover (Sverdrup, Johnson, and Fleming, 1946):

$$Q_b = (8.129 \times 10^{-11} (t_w + 273.15)^4 (0.255 + 0.32 \times 10^{-0.0006e_a})) (1 - 0.0083C) \quad (10)$$

Q_b was calculated at three hour intervals and then averaged to obtain daily means. Water temperatures were estimated by averaging stations 58-63 (Colton *et al.*, 1968) and air temperatures were taken from the data recorded at Portland airport (U.S. Weather Bureau).

The latent heat of evaporation, Q_e , was determined by the equations reported by Sverdrup, Johnson, and Fleming (1946) and Brown and Beardsley (1978). Data from Portland lightship (Chase, 1957 and 1969) and Portland airport (U.S. Weather Bureau) were used to calculate daily values of Q_e :

$$Q_e = EL \quad (11)$$

$$L = 596 - 0.52 t_w \quad (12)$$

$$E = 0.007 (e_w - e_a) W \quad (13)$$

$$e_w = e_t (1 - 5.37 \times 10^{-4} S) \quad (14)$$

The sensible heat loss, Q_h , was calculated using Bowen's ratio, B , (Bowen, 1926). Data from Portland lightship (Chase, 1967 and 1969) and Portland airport (U.S. Weather Bureau) were used to calculate daily values of Q_h :

$$Q_h = Q_e B \quad (15)$$

$$B = 0.49 \left(\frac{t_w - t_a}{e_w - e_a} \right) \quad (16)$$

Notations and Units Used

- B Bowen's ratio
 C % cloud cover
 E amount of water evaporated from the sea surface (gm cm⁻² d⁻¹)
 E_s maximum (noon) daily elevation of the sun (degrees)
 e_a actual water vapor pressure of air (mb)
 e_t saturated water vapor pressure of air at temperature of water surface for distilled water (mb)
 e_w saturated water vapor pressure of air at the temperature of the water surface, corrected for salinity (mb)
 h root mean square of the sun's maximum elevation (degrees)
 L latent heat (cal gm⁻¹)
 Q total heat exchange (gm cal cm⁻² d⁻¹)
 Q_b effective back radiation from the sea surface
 Q_d diffuse incoming sky radiation
 Q_e transfer of heat by evaporation
 Q_h convection of sensible heat
 Q_t total incoming radiation (solar and sky)
 Q_r reflection back from the sea surface

Q_s	direct solar radiation
r	reflectivity ratio
S	salinity (‰)
s	percent of total possible hours of sunlight
t_a	temperature of the air (°C)
t_w	temperature of the sea surface (°C)
W	wind speed (knots)

REFERENCES

- Beardsley, R. C., W. C. Boicourt, and D. R. Hansen. 1976. Physical oceanography of the Middle Atlantic Bight, in *Middle Atlantic Continental Shelf and the New York Bight*. L & O Special symposia, Vol. 2.
- Bigelow, H. B. 1927. Physical oceanography of the Gulf of Maine. U.S. Dept. of Comm. Bur. Fish Bull., 40, 511-1027.
- 1933. Studies of the waters on the continental shelf, Cape Cod to Chesapeake Bay. I. The cycle of temperature. *Pap. Phys. Oceanogr.*, 2, 135 p.
- Bowen, I. S. 1926. The ratio of heat losses by conduction and by evaporation from any water surface. *Phys. Rev.*, 27, 779-787.
- Brown, W. S. and R. C. Beardsley. 1978. Winter circulation in the western Gulf of Maine, Part I. Cooling and water mass formation. *J. Phys. Oceanogr.*, 8, 265-277.
- Bue, C. D. 1970. Streamflow from the United States into the Atlantic Ocean during 1931-60. U.S. Geol. Surv., Washington, D.C. Water-Supply Paper 1899-1. 36 pp.
- Bumpus, D. F. 1973. A description of the circulation on the continental shelf on the east coast of the United States. *Progr. Oceanogr.*, 6, 111-157.
- 1976. Review of the physical oceanography of Georges Bank. I.C.N.A.F. Res. Bull. No. 12.
- Bumpus, D. F. and L. M. Lauzier. 1965. Surface circulation on the continental shelf off eastern North America between Newfoundland and Florida. *Am. Geograph. Soc. Serial Atlas of the Mar. Environ. Folio 7*: 4 p., 8 pl., App.
- Bunker, A. F. 1956. Stress, turbulence, and heat flow measurements over the Gulf of Maine and surrounding land. ONR Technical Report #41, WHOI Reference No. 56-65. Unpublished Manuscript, p. 43.
- 1960. Heat and water vapor fluxes in air flowing southward over the western North Atlantic Ocean. *J. Meteor.*, 17, 52-63.
- 1972. Winter time interactions of the atmosphere with the Mediterranean Sea. *J. Phys. Oceanogr.*, 2, 225-238.
- Burt, W. V. 1953. A note on the reflection of diffuse radiation by the sea surface. *Trans. Amer. Geophys. Un.*, 34, 329.
- Chase, J. 1967. Oceanographic observations, 1964, east coast of the United States. U.S. Fish Wildl. Serv., Data Rep. 18, 177 pp.
- 1969. Oceanographic observations, 1965, east coast of the United States. U.S. Fish Wildl. Serv., Data Report 32, 156 pp.
- Colton, J. B., Jr. 1964. History of oceanography in the offshore waters of the Gulf of Maine. U.S. Fish and Wildlife Service, Special Scientific Report—Fisheries No. 496. 18 pp.
- 1968. Recent trends in subsurface temperatures in the Gulf of Maine and Contiguous waters. *J. Fish Res. Bd. Canada*, 25, 2427-2437.
- 1972. Temperature trends and the distribution of ground fish in continental shelf waters, Nova Scotia to Long Island. *Fish. Bull.*, 70, 637-657.
- Colton, J. B., R. R. Marak, S. Nickerson, and R. F. Stoddard. 1968. Physical, chemical, and

- biological observations on the Continental Shelf, Nova Scotia to Long Island, 1964-1966. U.S. Dept. Interior, FWS Data Rept. 23, Washington, D.C.
- Drinkwater, K. F., and W. H. Sutcliffe, Jr. 1977. Seasonal geostrophic volume and salt transports over the Scotian Shelf. Submitted to J. Fish. Res. Bd. Can.
- Gatien, M. G. 1976. A study in the slope water region south of Halifax. J. Fish Res. Bd. Canada, 33, 2213-2217.
- Greenberg, D. A. 1977. Mathematical Description of the Bay of Fundy—Gulf of Maine numerical model. Marine Environmental Data Service Technical Note No. 16, 20 pp.
- Hayes, R. M. 1975. Oceanographic observations, Nova Scotia to Cape Hatteras, North Carolina, October-November 1969 and May-June 1970. U.S. Coast Guard Oceanogr. Unit, Oceanogr. Rept. #CG 373-66, 239 pp.
- Hopkins, T. S. 1976. Coastal cooling in the Gulf of Maine. Bigelow Laboratory for Ocean Sciences. Contribution #76-033.
- 1978. Physical processes in the Mediterranean Basins, in *Transport Processes in Estuarine Environments*, B. Kjerfve, ed., University of South Carolina Press.
- Hopkins, T. S. and N. Garfield. 1978. Physical oceanography, in *A Summary of Environmental Information, Continental Shelf, Bay of Fundy to Cape Hatteras*. Center for Natural Areas, Washington, D.C. 1(2): IV-1 to IV-170.
- Lee, A. H. 1970. The T-S structure, circulation and mixing in the Slope Water region east of the Scotian Shelf. Ph.D. Thesis, Dalhousie University, Halifax, N.S. 191 p.
- McLellan, H. J. 1957. On the distinctness and origin of the Slope Water off the Scotian Shelf and its easterly flow south of the Grand Banks. J. Fish. Res. Bd. Canada, 14, 213-239.
- Meade, R. H. 1971. The Coastal Environment of New England. New England River Basins Commission, Boston. 47 pp.
- National Marine Fisheries Service. 1976. Unpublished cruise data. Woods Hole, Massachusetts.
- Neumann, G. and W. J. Pierson, Jr. 1966. Principles of Physical Oceanography, Prentice-Hall, Inc., Englewood Cliffs, N.J. 545 pp.
- Pawlowski, R. J. 1977. March 1977 temperature transect for the Gulf of Maine. National Marine Fisheries Service, 2-7, 4/17/77.
- Saunders, P. M. 1977. Wind stress on the ocean over the eastern continental shelf of North America. J. Phys. Oceanogr., 7, 555-566.
- Shuleikin, V. V. 1959. Kratkii kurs fiziki morya. Gidromet. Idat, Leningrad. 478 pp.
- Speirs, G. D., J. J. Graham, and R. L. Dow. 1976. Forecasting availability of juvenile herring along the Maine coast: a project and report to the Maine Sardine Council. Dept. Mar. Res., W. Boothbay Harbor, Me. Unpublished Manuscript.
- Sutcliffe, W. H., Jr., R. H. Loucks, and K. F. Drinkwater. 1976. Coastal circulation and physical oceanography of the Scotian shelf. J. Fish. Res. Bd. Canada, 33, 98-115.
- Sverdrup, H. V., M. W. Johnson, and R. H. Fleming. 1946. The Oceans, Their Physics, Chemistry, and General Biology. Prentice-Hall, Englewood Cliffs, N.J. 1087 pp.
- Swallow, J. C. and G. F. Caston. 1973. The preconditioning phase of MEDOC 1969-I, Observations. Deep-Sea Res., 20, 429-448.
- Trites, R. W. and R. E. Banks. 1958. Circulation on the Scotian Shelf as indicated by drift bottles. J. Fish Res. Bd. Canada, 15, 79-89.
- U.S. Weather Bureau. Published monthly. Local climatological data, Portland, Maine. U.S. Dept. Comm., Weather Bureau, Washington, D.C.
- Wright, W. R. and C. E. Parker. 1976. A volumetric temperature/salinity census for the Middle Atlantic Bight. Limnol. Oceanogr., 21, 563-571.